Article

Improving the Energy Efficiency of a Ship's Power Plant by Using an Autonomous Hybrid System with a PMSG

Dariusz Tarnapowicz [1,*], Sergey German-Galkin [1], Arkadiusz Nerc [1] and Marek Jaskiewicz [2]

1 Faculty of Mechatronics and Electrical Engineering, Maritime University of Szczecin, 70-500 Szczecin, Poland
2 Faculty of Mechatronics and Mechanical Engineering, Kielce University of Technology, 25-314 Kielce, Poland
* Correspondence: d.tarnapowicz@pm.szczecin.pl; Tel.: +48-9148-09-955

Abstract: In ship systems, diesel power generators are used in various systems of autonomous power plants to ensure power supply security. This article presents an autonomous hybrid system of a ship power plant with a diesel generator with a permanent magnet synchronous generator and electricity storage in parallel topology (the permanent magnet synchronous generator is connected directly to the receiving network). The electricity storage through the active converter is connected to the receiving network in parallel with the permanent magnet synchronous generator. The decoupled control of the reactive and active power in the active converter enables stabilization of the voltage in the ship's electrical power grid while ensuring the possibility of obtaining different operating regimes of the power plant at various stages of the ship's operation. The innovative method of voltage stabilization presented in this article is based on the compensation of the unfavorable reaction of the permanent magnet synchronous generator armature through the optimal transmission of negative inductive reactive power from the active converter to the generator using the electromagnetic properties of the synchronous generator. The active converter controls the direction of the active power transmission between the DC source, the grid, and the permanent magnet synchronous generator. This paper proposes a hybrid autonomous power plant system using battery storage in place of a single diesel generator set against the commonly used two diesel generator sets, working in parallel, to increase the energy efficiency of the power plant by minimizing the specific fuel consumption of the diesel generator set. The article examines the possibilities of such a mechatronic system design based on analytical research and analysis of electromagnetic and energy characteristics using the Matlab-Simulink program.

Keywords: energy efficiency; diesel generator; permanent magnet synchronous generator; voltage control; hybrid power system; ship power plant; power transmission

1. Introduction

The growing demand for electricity on ships, combined with environmental sustainability, poses new challenges for engineers in the design of electricity generation systems.

In ship power grids, the basic source of electricity is a diesel-generating (DG) set with an external excitation synchronous generator (EESG). This energy source is used in about 80% of solutions [1]. The main task of a ship power plant is to ensure high-quality electricity but also continuity and reliability of the power supply.

In recent years, great emphasis has been placed on increasing ship energy efficiency in economic and environmental terms (e.g., reducing air pollutant emissions, especially in the port). The regulations of the International Maritime Organization, primarily the introduction of the Energy Efficiency Design Index (EEDI) [2,3], pose a great challenge to engineers who, in order to improve EEDI, search for solutions using new technologies or by increasing the energy efficiency of systems currently used on board. This fact made the permanent magnet synchronous generator (PMSG) displace the EESG in power range from a few kilowatts to several dozen megawatts in the increasingly newer categories of

devices—in energy, land, marine, and aviation technologies. There are more and more companies installing PMSGs on vessels. This is mainly due to the high reliability of these machines, good energy efficiency, reduced weight, and dimensions [4,5].

In recent years, hybrid mechatronic systems with PMSGs are widely used in generating sets of autonomous objects, such as hybrid electric vehicles [6–8], wind turbines [9–11], airplanes [12–14], and marine generating sets [15,16].

The voltage at the output of a constant-speed PMSG depends on the load, which is explained by a phenomenon that in electromechanics is called "armature reaction". In order to maintain a constant voltage value in the network, serial power electronic topologies are commonly used (mainly in wind turbine systems) [17–19]. In Figure 1, an autonomous hybrid power plant system with the PMSG in series topology is presented.
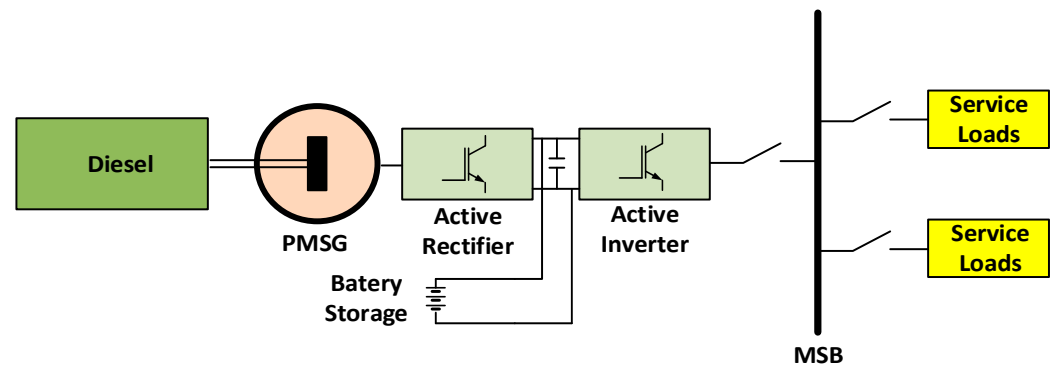
Figure 1. Typical autonomous hybrid power plant system with the PMSG in series topology.

The main disadvantage of the system in the serial topology (Figure 1) is the reduction in reliability. In the event of a failure of the power electronic system, there is no power supply to the utility consumers, which in turn leads to a reduction in the safety of the ship's operation.

Therefore, the authors propose a parallel topology system (Figure 2).
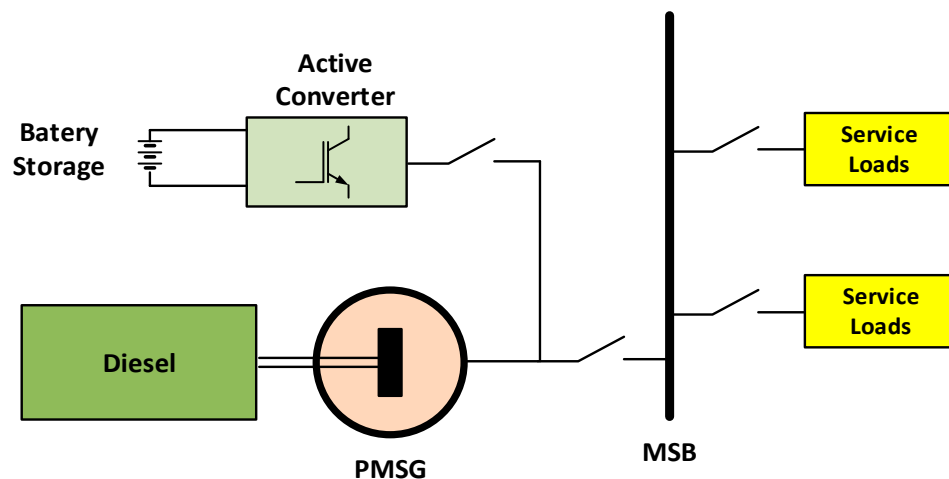
Figure 2. Autonomous hybrid power plant system with the PMSG in parallel topology.

There are various solutions for implementing parallel topology [20,21] with voltage stabilization in the receiving network characterized by a complicated control algorithm. The topology presented in this article is similar to STATCOM systems (STATic COMpensator) and active filters [22,23]. The difference is that reactive power compensation is not the main goal, as in STATCOM, but the electromagnetic properties of the PMSG (compensation of the unfavorable armature PMSG) are used. All reactive inductive power is sent to the load grid (whose loads are primarily squirrel-cage motors) and to the PMSG for voltage stabilization [24].

In currently used marine generating sets with EESG, the active electric power at the output is maintained by the diesel engine rotational speed controller, and the output reactive electric power is maintained by the excitation voltage regulator of the generator itself. In the case of using the PMSG as an electric generator, it is not possible to regulate the excitation voltage, which causes a voltage drop at the generator output with increasing load. The idea of compensating the voltage drop at the PMSG output, proposed in this article, is based on the generation of negative (capacitive) reactive power, which is provided by an active converter (AC) connected in parallel with the PMSG to a common load (Figure 2).

One of the ways to reduce the emission of air pollutants by ships moored in ports is the "Shore to Ship" system [25], which enables switching off of the DG's ship power generators and connecting the ship's power system to the shore power supply. However, this system requires technologically advanced devices installed in the port, which are not yet widely used. The ship power plant hybrid system proposed in this article makes it possible to switch off the DG units in the port and switch to the power supply from the ship's energy storage in the absence of the "Shore to Ship" system in the port.

This article presents an analysis of the operation of a hybrid marine power plant system, which will operate in five basic modes:

I. Maneuvers of the vessel at port entry (port exit). According to the regulations of the qualification societies, parallel operation of two autonomous sources of electricity is required [1,26].

II. Sea voyage of a ship—short-term (about a dozen or so minutes, 3 times a day) dynamic load change. This occurs when a large load (e.g., start-up air compressor) is turned on. When the load of one generating set is high (e.g., 70%), in commonly used solutions, the second generating set is switched on for parallel operation.

III. Sea voyage of the ship—stable load of the power plant. This is the period that lasts the longest during the ship's contract. One DG generating set is in operation.

IV. Ship's sea voyage—stable power plant load and battery charging (if necessary).

V. Stopover in the port. DG's generating sets are switched off in order to reduce the emission of air pollutants. Electricity is provided by the battery system.

The main problem of increasing the energy efficiency of ship systems is difficult for ship system designers to achieve.

Among optimization (energy optimization) techniques, several categories can be distinguished [27] such as conventional optimization, genetic optimization [28], artificial intelligence [29,30], and new bio-inspired algorithms [31–33].

The specifics of the ship's power plant do not allow the use of optimization techniques used on land. This is due to limitations related primarily to the operating condition of the internal combustion engines driving the DG set. This can be explained by the example of the PMS (power management system) commonly used on ships. When one DG unit is operating and the load is increasing, then after exceeding a certain value (e.g., 70% of the rated load), the second DG set is switched on for parallel operation. The value (which is variable) at which the second unit will turn on is decided by the engineer officer and is related to the operating condition of the combustion engine of the DG set.

Empirical studies on ships prove that the maximum load on the internal combustion engines of DG sets is about 65–75% [34].

A second example of common shipboard solutions is the asymmetric operation of two DG sets. The mechanical officer selects the maximum possible load for one unit due to the condition of the unit's internal combustion engine.

In both examples shown, the fuel consumption of the DG sets is minimal for the current condition of the internal combustion engine. This can be seen in the characteristics of specific fuel consumption as a function of load P [34].

The authors of this article propose to increase efficiency by operating two DG units in parallel. However, instead of the commonly used system of two DG units in parallel operation, one DG unit and battery storage are used in a hybrid system with asymmetric loading of the sources. In the commonly used system, the load on the DG units is small

(e.g., during shunting 25% of the rated power [1]) with a very high SFC (specific fuel consumption) [34]. In the proposed solution, the load on one DG unit will be higher with a reduced SFC factor (e.g., during shunting 50% of the rated power.

The authors of this article propose the use of the PMSG generator set using a new voltage stabilization method instead of the EESG generator sets commonly used on ships. The use of the PMSG in place of the EESG due to the properties mentioned earlier increases the energy efficiency of the system. The authors examined the effectiveness of the new voltage stabilization method in different ship operation modes.

The article is organized as follows:

Section 2 introduces the electrical energy storage that is proposed in the studied autonomous hybrid system from the PMSG of the ship's power plant. Then, the details of the AC control analysis of the system based on the use of the physical properties of the system that realizes the stabilization of the grid voltage in a novel way in different operating states of the ship are discussed.

Section 3.1. presents the analytical results of the autonomous hybrid system from the PMSG system, confirming the adopted analysis.

Section 3.2. presents the results of simulation tests of the autonomous hybrid system from the PMSG system for various operating states of the ship, confirming the analytical results.

The article concludes in Section 3 with a commentary on the obtained results.

Section 4 summarizes the proposed system's performance in stabilizing the grid voltage and improving the energy efficiency of the ship's power plant.

2. Methods

In terms of reducing greenhouse gas emissions by ships mooring in the port, the proposed autonomous hybrid ship power plant system includes an electricity storage facility that will provide power to the ship in the port.

Until recently, electrical energy storage based on maintenance-free VRLA (valve-regulated lead acid) batteries was widely used in marine systems. A variation of lead-acid batteries used in the shipbuilding industry was gel batteries, which operate in any position due to their immobile gelatin electrolyte.

Lithium-ion batteries are the latest evolution of battery power, offering a range of applications for shipowners. The main advantages of lithium-ion batteries used in the marine industry are:

- Lighter than lead-acid batteries,
- High performance,
- Long cycle life,
- High energy density,
- High power density.

This article proposes energy storage based on lithium-ion batteries.

Dimensioning of the batteries used in the system depends primarily on the type of ship (e.g., bulk carrier, container carrier, gas carrier, and ferry) and its size (vessel load capacity) [35], and the time of stay in the port. The Table 1. shows an example of electricity consumption by ships mooring in the port and the weight of the required battery system (marine lithium-ion battery) [1,35].

Table 1. Energy consumption on a ship in port and battery storage weight [1,35].

Vessel Type	Bulk	Bulk	RoRo	Container
Size [DWT]	30 k	80 k	20 k	50
Duration [h]	12	12	10	10
Power [kW]	180	250	1000 k	2000 k
Energy consumption [MWh]	2.1	3	10	20
Battery weight (Cell level) [T]	12.6	18	60	120

Each ship at the time of design has a power balance performed for the primary sources of electricity. The power balance is performed in 4 modes of operation of the ship: voyage of the ship at sea, maneuvering, berthing in the port, and berthing in the port with a transshipment using the ship's equipment.

In the example discussed in this article, a berth in port with a transshipment was assumed to have a peak load of 1.5 MW. For the selection of the battery storage, the average duration of the ship's standstill in the port is important. In the example discussed here, a berth of 10 h was assumed. The energy consumption of the battery storage, in this case, is 15 MWh. Using the specific weight for lithium-ion batteries (Cell level) SW = 6 kg/kWh [35], the weight of the battery storage in the case at hand is 90 T.

The autonomous hybrid system with the PMSG control method proposed in the article, using decoupled AC control, will allow stabilization of the voltage in the ship's network (reactive power control) and optimal loading of the DG unit with the lowest specific fuel consumption (active power control).

AC control is based on the analysis of steady-state PMSG operation using the field-oriented control method [17,18].

When the PMSG is used as an electric generator, it is not possible to regulate the excitation voltage, which causes the generator output voltage to drop as the load increases. The compensation of this voltage drop was analyzed based on the block diagram shown in Figure 2.

When developing a control algorithm for a converter designed for variable load operation, it was proposed that the control of the converter would be implemented in a system with negative current feedback [36–38]. This control has been called "current control". In this case, the electromagnetic and energetic processes in the system can be studied on the basis of the equivalent circuit shown in Figure 3.
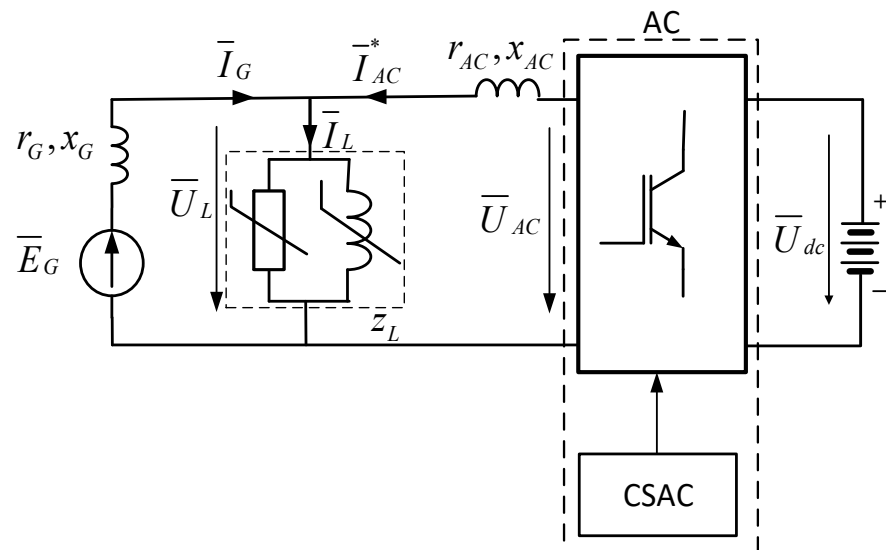
Figure 3. Equivalent circuit of a generator set with the PMSG.

In the substitute circuit shown, the active converter (AC) is connected in parallel to the load (Z_L) and windings of a synchronous generator with a constant rotational speed and immutable electromotive force ($\overline{E}_G = p\omega_m\psi_0 = const$). Resistance and reactance (r_G, x_G) in the equivalent circuit are internal parameters of the PMSG. The mathematical description of the "AC-PMSG" system in the coordinate system rotating synchronously with the machine shaft can be presented as:

$$\begin{aligned}
\overline{E}_G(t) &= \overline{U}_L(t) + L\frac{d\overline{I}_G(t)}{dt} + r_G\overline{I}_G(t) + jx_G\overline{I}_G(t), \\
\overline{I}_L(t) &= \overline{I}_G(t) + \overline{I}_{AC}(t)
\end{aligned} \tag{1}$$

where:

$\overline{E}_G(t)$—space vector (resultant) EMF of the generator stator windings;
$\overline{U}_L(t)$—resultant vector of the load voltage;
$\overline{I}_G(t)$—the resultant vector of the current in the armature of the PMSG;
$\overline{I}_{AC}(t)$—the resultant vector of the first harmonic of the current generated by the AC;
$\overline{I}_L(t)$—the resultant vector of the current in the load;
$x_G = wL_G$—reactance of the PMSG;
r_G—resistance of the PMSG.

Note that the notation $\overline{E}_G(t), \overline{U}_L(t), \overline{I}_G(t), \overline{I}_{AC}(t)$, etc., in the equations emphasizes the fact that these quantities are constantly changing with the time. During the transient processes, changes in the values of currents, voltages, and the electromotive force are observed.

In the steady state, the system of Equation (1) is transformed into the following form:

$$\begin{aligned} \overline{E}_G &= \overline{U}_L + r_G\overline{I}_G + jx_G \cdot \overline{I}_G, \\ \overline{I}_L &= \overline{I}_G + \overline{I}_{AC} \end{aligned} \tag{2}$$

Further, in accordance with Equation (2), vector diagrams were constructed in all possible operating modes of the system, which allow for a preliminary (qualitative) assessment and selection of the operating mode of the system. This enables the stabilization of the output voltage under load to be secured.

Figure 4 shows vector diagrams for two operating modes of the "AC-PMSG" system, in which the active converter compensates for the reactive component of the load current.

(**a**)   (**b**)
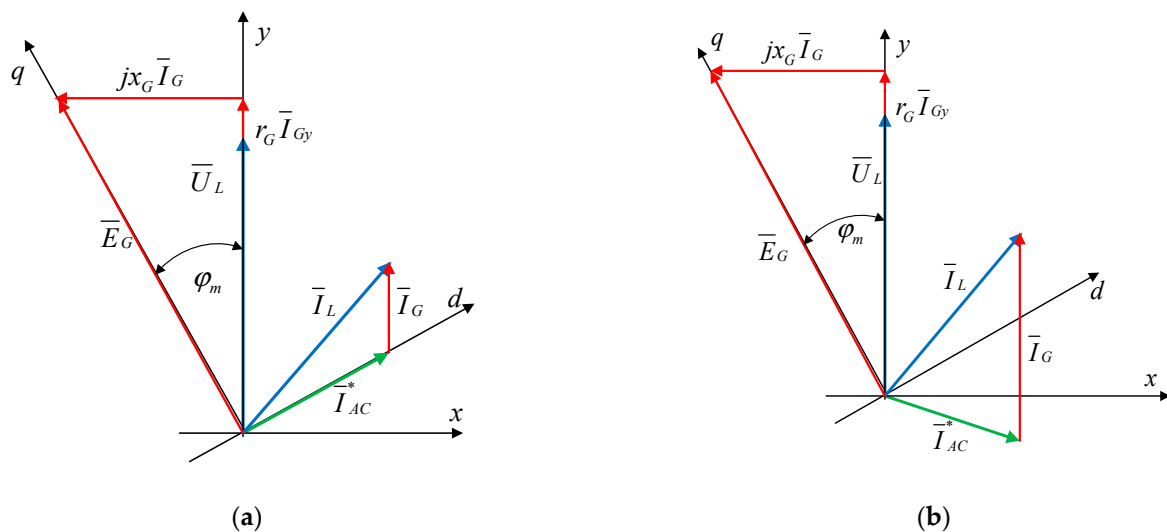
Figure 4. Vector diagrams of the system with load compensation with an active converter generating active and reactive currents (active and reactive powers): (**a**) The load current is the sum of the generator current and the current of AC. (**b**) the PMSG current feeds the load and charges the battery in the DC circuit. (red vectors—refer to PMSG, blue vectors—refer to load, green vectors—refer to AC).

In the first mode (Figure 4a), the active load current is the sum of the generator current and the AC. In the second mode (Figure 4b), the PMSG generates a current that powers the load and charges the battery in the DC circuit. The active load current in this case is taken only from the generator.

Vector diagrams in which the AC generates only reactive power to the system are shown in Figure 5. In the first case (Figure 5a), the AC fully compensates for the reactive power of the load. In the second case, the AC generates a reactive current greater than the current required by the load. In this case, the generator is loaded with negative (capacitive) reactive power.

(**a**) (**b**)
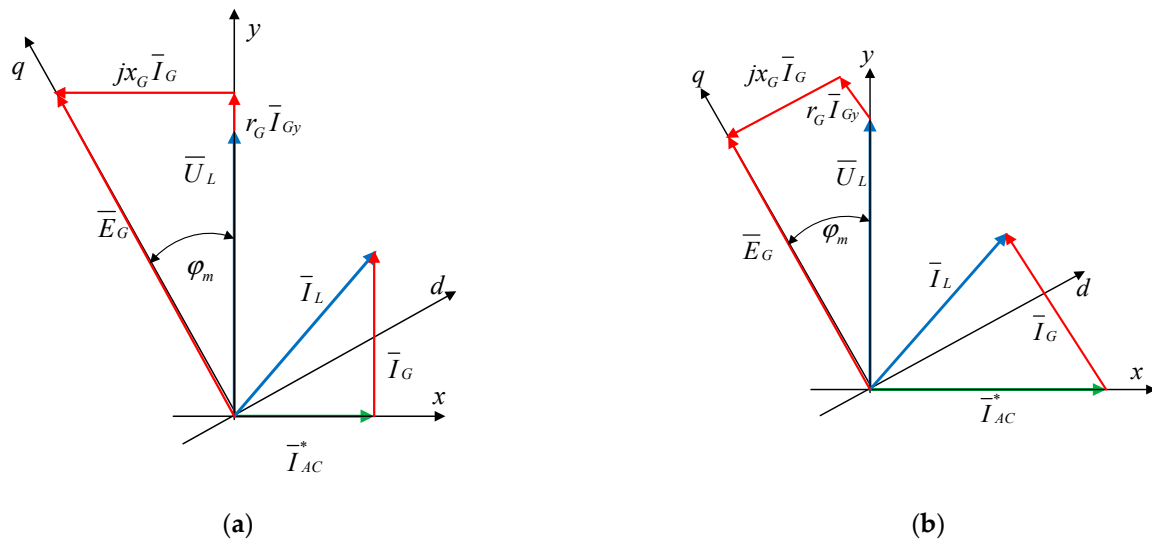
Figure 5. Vector diagrams of the system with load compensation with an active converter generating only reactive current (reactive power): (**a**) The AC fully compensates for the reactive power of the load, (**b**) AC case generates reactive current greater than the current required by the load; the generator is loaded with negative (capacitive) reactive power. (red vectors—refer to PMSG, blue vectors—refer to load, green vectors—refer to AC).

The vector diagrams shown in Figures 4 and 5 allow for the selection of the operating mode that ensures the stabilization of the output voltage in the system under variable load. Based on the requirement for a constant voltage on the load when changing the operating mode of the generator from no load to the maximum value, this requirement is reduced to equality $E_G = U_L = const$. This mode of operation is only provided in the case shown in Figure 5b. The use of a size and phase-controlled current source $\overline{I}_{AC}^*$ maintains a constant voltage in the electrical network for the load changes due to the generation of negative (capacitive) reactive current.

The vector Equation (2), written in complex form, can be converted into equations in the axes by taking the x axis as the real axis and the y axis as the imaginary axis and combining the voltage on the load with the imaginary y axis, $\overline{E}_G = \overline{E}_{Gx} + j\overline{E}_{Gy}, \overline{U}_L = j\overline{U}_{Ly}, \overline{I}_G = \overline{I}_{Gx} + j\overline{I}_{Gy}, \overline{I}_L = \overline{I}_{Lx} + j\overline{I}_{Ly}, \overline{I}_{AC}^* = \overline{I}_{ACx}^*$; therefore, Equation (2) can be rewritten as:

$$
\begin{aligned}
\overline{I}_{Gx} &= \overline{I}_{Lx} - \overline{I}_{ACx}^*, \\
\overline{I}_{Gy} &= \overline{I}_{Ly} - \overline{I}_{ACy}^*, \\
\overline{E}_{Gx} &= r_G \overline{I}_{Gx} - x_G \cdot \overline{I}_{Gy}, \\
\overline{E}_{Gy} &= \overline{U}_L + x_G \overline{I}_{Gx} + r_G \overline{I}_{Gy}.
\end{aligned}
\tag{3}
$$

According to Equation (3), an extensive vector diagram was constructed (Figure 5) from which geometric dependencies, taking into account the equality, $E_G = U_L = const$, electromagnetic, and energy characteristics of the system, are calculated:

$$
\begin{aligned}
I_{AC}^* &= I_{Lx} + I_{Gx}, \\
I_{Gy} &= I_{Ly}, \\
E_{Gx} &= r_G I_{Gx} + x_G \cdot I_{Gy}, \\
E_{Gy} &= U_L - (x_G I_{Gx} - r_G I_{Gy}), \\
U_L &= \sqrt{E_{Gx}^2 + E_{Gy}^2}.
\end{aligned}
\tag{4}
$$

From Equation (4), the longitudinal component of the generator current and the control current is determined where the voltage on the load is constant:

$$
\begin{aligned}
I_{Gx} &= \frac{U_L}{z_g} - \sqrt{\left(\frac{U_L}{z_G}\right)^2 - I_{Ly}^2}, \\
I_{AC}^* &= I_{Lx} + I_{Gx}.
\end{aligned}
\tag{5}
$$

where $z_g = \sqrt{r_G^2 + x_G^2}$—the generator's own impedance.

Equations (4) and (5) enable calculation of the energy characteristics of the system:

$$
\begin{aligned}
P_L &= 1.5 U_L I_{Ly},\, Q_L = 1.5 U_L I_{Lx}, \\
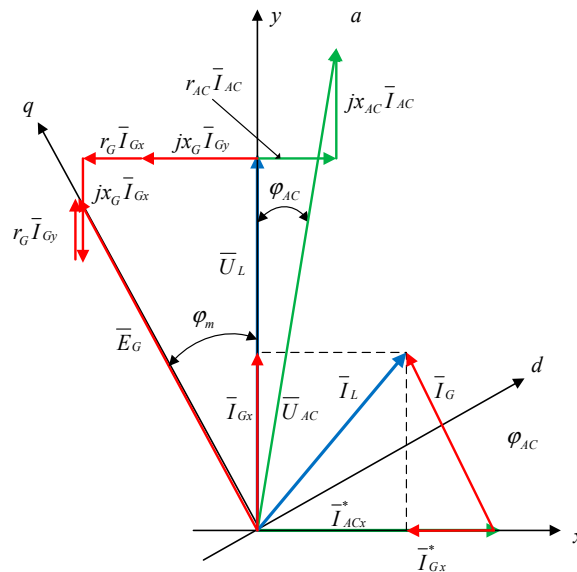P_G &= 1.5 U_L I_{Gy} = 1.5 U_L I_{Ly}, \\
Q_G &= 1.5 U_L I_{Gx} = 1.5 U_L (I_{AC}^* - I_{Lx}), \\
P_{AC} &= 1.5 U_{ACx} I_{AC}^* = 1.5 U_{AC} I_{AC}^* \sin\varphi_{ac}, \\
Q_{AC} &= 1.5 U_{ACy} I_{AC}^* = U_{AC} I_{AC}^* \cos\varphi_{ac},
\end{aligned}
\tag{6}
$$

where φ_{ac} is determined on the basis of geometrical structures of a vector diagram (Figure 6).

$$
\varphi_{AC} = arctg \frac{r_{AC} I_{AC}^*}{U_L + x_{AC} I_{AC}^*}
\tag{7}
$$

Figure 6. Vector diagram of electromagnetic processes in a power generator. (red vectors—refer to PMSG, blue vectors—refer to load, green vectors—refer to AC).

In common ship power plant systems, a single DG set is most often operated in mode III (floating at sea) and the designed power of DG is selected from the Ship's Power Balance. Empirical measurements of DG load indicate that in this mode the load is about 50–60% of the nominal load of the DG set. In mode II (maneuvering), two DG assemblies must be operated in parallel for safe exploitation. Empirical measurements of the DG load in this mode indicate that the load is about 25% of the nominal load of one DG set. This is very unfavorable for the propulsive internal combustion engines of the DG set, which are characterized by low energy efficiency [34] and the formation of the "wet stacking" phenomenon [17]. The results of the analysis of the control of the hybrid system (Figure 7) based on the vector diagram of electromagnetic processes in a power generator (Figure 6) show that the system can realize all five modes of operation of the ship (mentioned in the introduction) at the optimal load of the DG-PMSG unit.
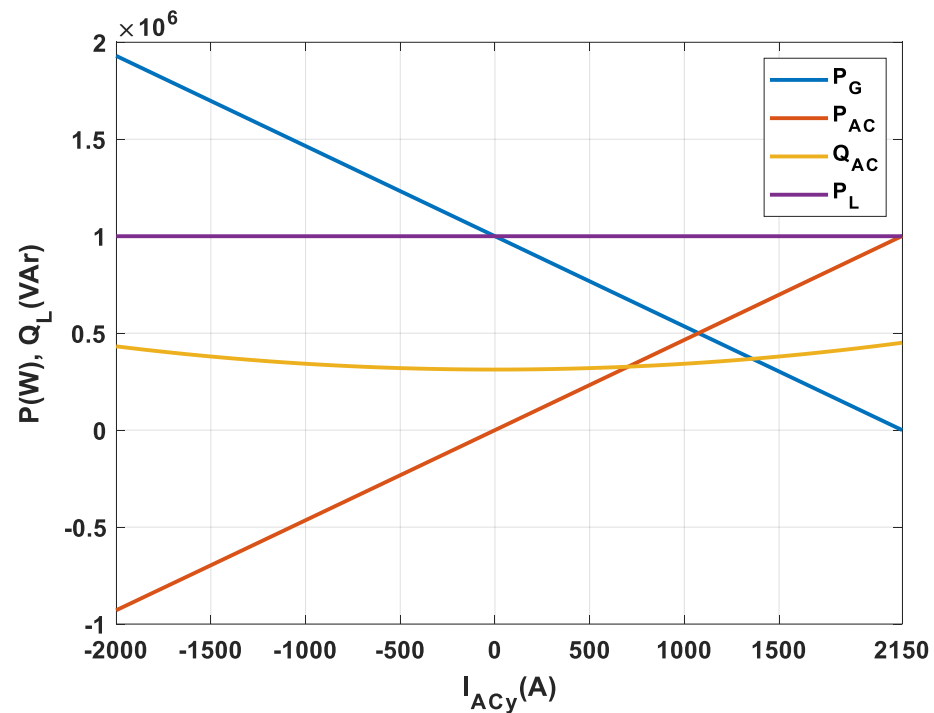
Figure 7. Energy characteristics of the network energy consumption optimization system.

3. Results

Analytical and simulation studies were carried out for a hybrid system of a ship power plant with the PMSG in parallel topology. The PMSG parameters are provided in Table 2.

Table 2. PMSG parameters.

P_G	U_N	n	r_G	L_G	ψ_0	p	m
MW	V	RPM	Ω	H	Vc	-	-
2	230	1500	0.0002	0.0000635	1.045	2	3

3.1. Results of Analytical Studies

The energy characteristics for the state of optimal power consumption from the PMSG in the tested hybrid system, calculated according to Equation (6), are shown in Figure 7. The dependence of the active power P_G of the generator, active power P_{AC}, and reactive power Q_{AC} AC as well as the active power of the load P_L depending on the converter's control current I_{ACy} are depicted.

The active power of the load P_L is the sum of the power drawn from the P_G generator and the active power of the P_{AC} battery. For the negative control current $I_{Acy} < 0$ positive active power of the load P_L, the battery is charged in the DC circuit. For $I_{Acy} > 0$ positive load active power P_L, the battery in the DC circuit is discharged. For $I_{Acy} = 0$ positive load active power P_L, the battery is neither charged nor discharged. The power is the sum of the power drawn from the mains and the battery. When the current value $I_{Acy} = 2150$ A, all the active power of the load P_L is taken from the batteries $P_L = P_{AC}$ (stopover in the port).

At the set active and reactive power of the load $I_{Lx} = \frac{Q_L}{1.5U_1}$, $I_{Ly} = \frac{P_L}{1.5U_1}$, the control current of the active converter is constructed in accordance with Equation (5). This dependence is in fact the AC control characteristic shown in Figure 8. The projections of the calculated surfaces on the main plane show the AC control constant current lines, which indicate that this current depends on the active power and reactive power of the load (P_L i Q_L).
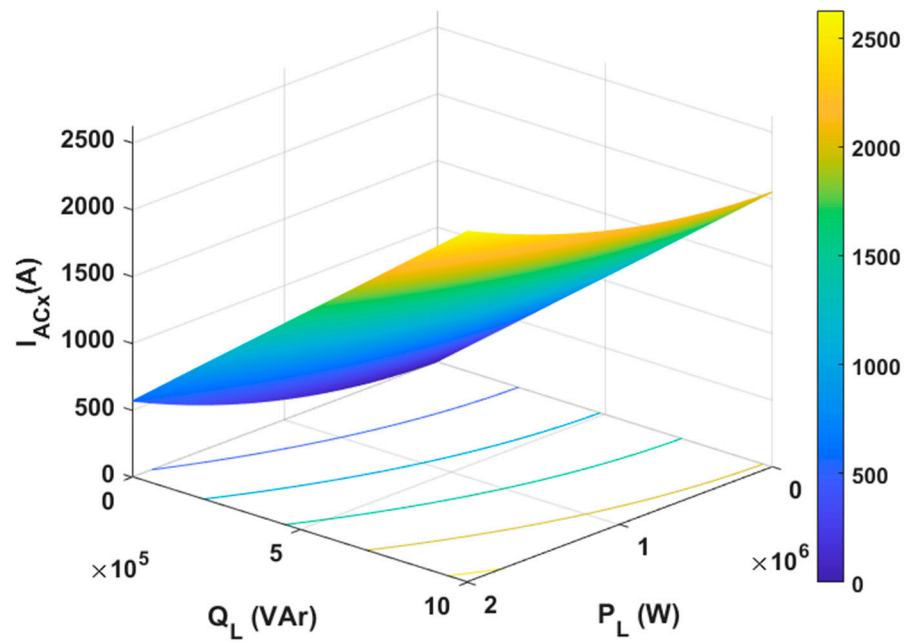
Figure 8. AC control characteristic.

After the angle φ_{AC} is obtained on the basis of the geometrical constructions of the vector diagram (Figure 6), the control vectors for the active converter are calculated from the equations:

$$
\begin{aligned}
I_{ACy} &= I_{AC}\sin(\varphi_{AC}), \\
I_{ACy} &= I_{AC}\cos(\varphi_{AC}).
\end{aligned}
\tag{8}
$$

The results of the calculation of the energy characteristics of the system are shown in Figures 9 and 10.
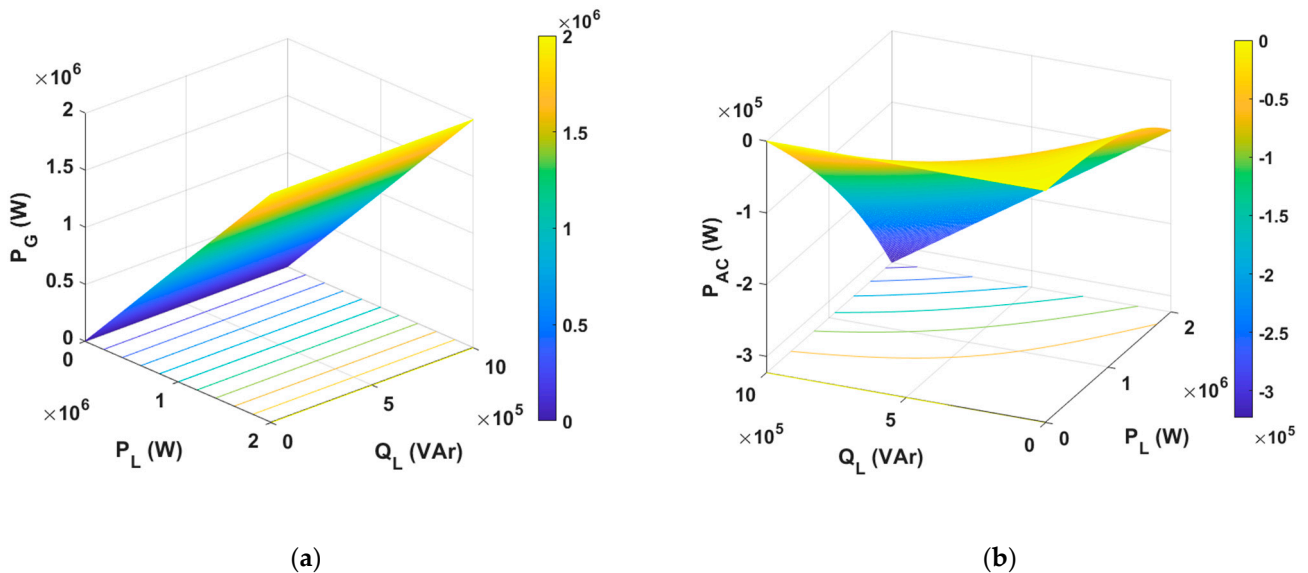

(**a**)

(**b**)

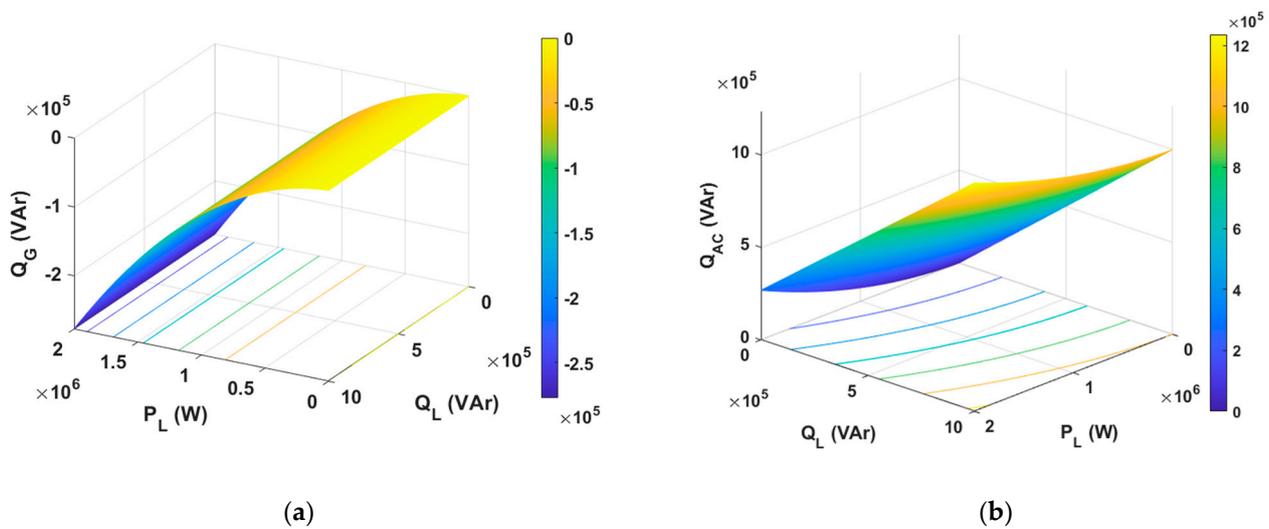**Figure 9.** Active power in the generator (**a**) and active converter (**b**).

Figure 10. Reactive power in the generator (**a**) and active converter (**b**).

As can be seen in Figure 9, the active power of the generator depends on the active power of the load and not on the reactive power of the load. The active power of the active converter increases with the increase in the active and reactive power of the load.

The results in Figure 10 show the dependence of the generator's reactive power only on the active power of the load and an upward trend of the reactive power of the active converter on the active and reactive power of the load.

3.2. Simulation Tests Results

Validation of analytical tests was carried out in simulation tests using the Matlab-Simulink program.

Figure 11 shows a schematic diagram of a hybrid system of a marine power plant with the PMSG in parallel topology together with the control system.
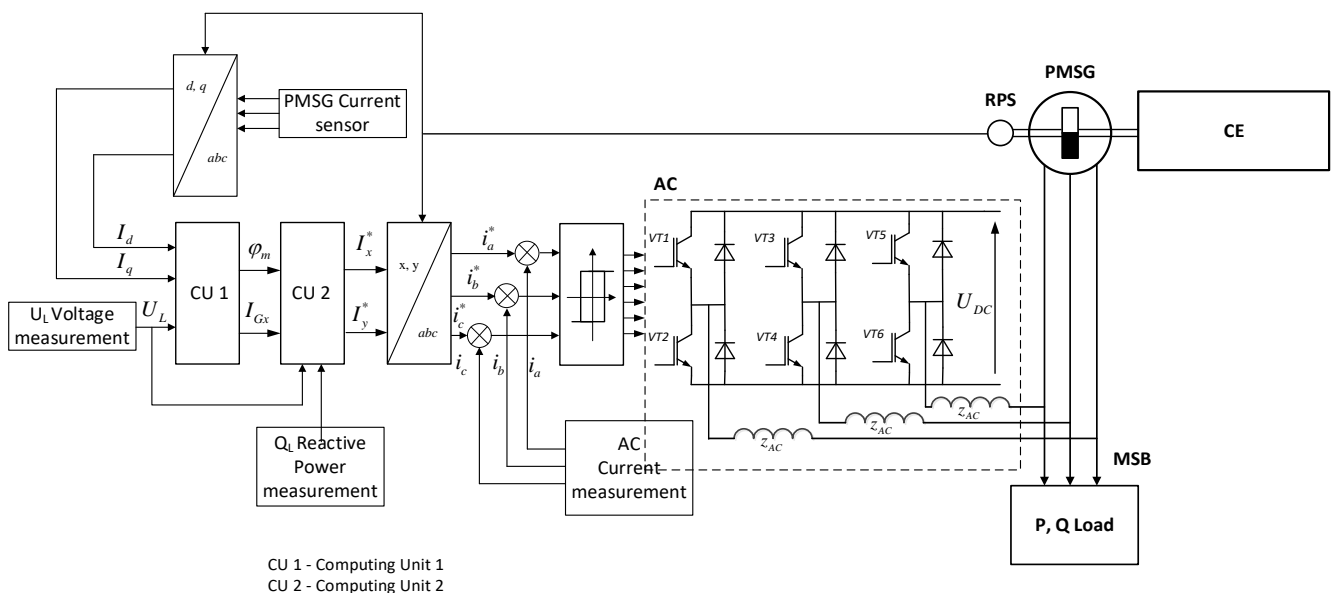

Figure 11. Autonomous hybrid ship power plant system with the PMSG in parallel topology with the control system.

The system includes, among other things:

- CE—combustion engine with speed regulator,
- PMSG—rare-earth magnet synchronous generator on the rotor,
- AC—active convertor,
- RPS—rotor position sensor,
- P,Q Load—variable load,
- CU 1—computer unit in which φ_m, I_{Gx} is determined,
- CU 2—computer unit in which I_x^*, I_y^* is determined,
- MSB—main switch board.

The AC is controlled from the rotor position sensor (Figure 11), which is installed in such a way that the emf of the machine $\overline{E}_G$ coincides with the imaginary q axis perpendicular to the magnetic flux, which is offset from the y axis by angle φ_m. This angle for $E_G = U_L = const$ results from the geometrical relationships of the vector diagram (Figure 6):

$$\varphi_m = \arcsin \frac{r_G I_{Gx} + x_G \cdot I_{Gy}}{U_L} \tag{9}$$

The electromagnetic processes in the load and the active converter are described on the x, y axes, and the electromagnetic processes in the generator on the *d, q* axes. The dependency between the currents in these axes is described by the Park–Gorev equations [39,40]:

$$\begin{aligned} I_d &= I_x \cos \varphi_m + I_y \sin \varphi_m, \\ I_q &= -I_x \sin \varphi_m + I_y \cos \varphi_m. \end{aligned} \tag{10}$$

An analogous relationship also holds for voltages. Based on the analysis, a model of the system was built (Figure 11) and implemented in the Matlab-Simulink program (Figure 12).
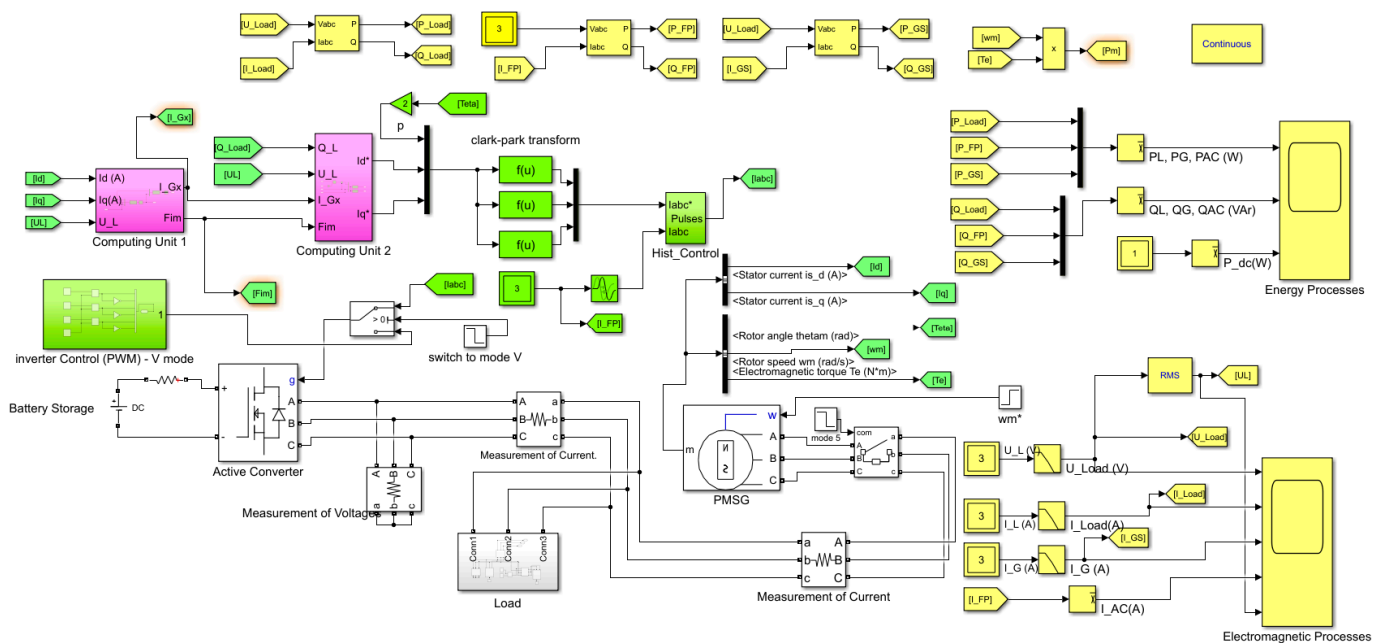
Figure 12. Autonomous hybrid ship power plant system with PMSG in parallel topology with the control system. Model implemented in the Matlab-Simulink program.

There are two main modules in the model that implement the proposed control algorithm:

Computer Unit 1: on the basis of measurements of currents in the *d, q* axes of the synchronously rotating coordinate system and measurement of the voltage in the U_L load

network using the trigonometric relationships shown in the PMSG—AC vector diagram (Figure 6), the angle φ_m and generator current in the x axis (I_{Gx}) are determined

Unit 2: on the basis of the determined angle φ_m, the determined generator current I_{Gx} in unit 1 and the determined reactive power Q_L and the measurement of the voltage in the load network U_L using the trigonometric relations shown in the PMSG—AC vector diagram (Figure 6), the setpoint currents in the d, q axes ($I_d{}^*$ and $I_q{}^*$) are determined.

Based on the calculated setpoint currents $I_d{}^*$ and $I_q{}^*$, through the inverse Clark–Park transform, the setpoint currents $I_{abc}{}^*$ are compared with the actual currents I_{abc} in the hysteresis block realizing control signals for the AC.

Figure 13 shows the electromagnetic and energy processes in a power generator without AC, where the change in voltage U_L for a time-varying load (P_L) is visible. All the active power P_G is sent to the load.
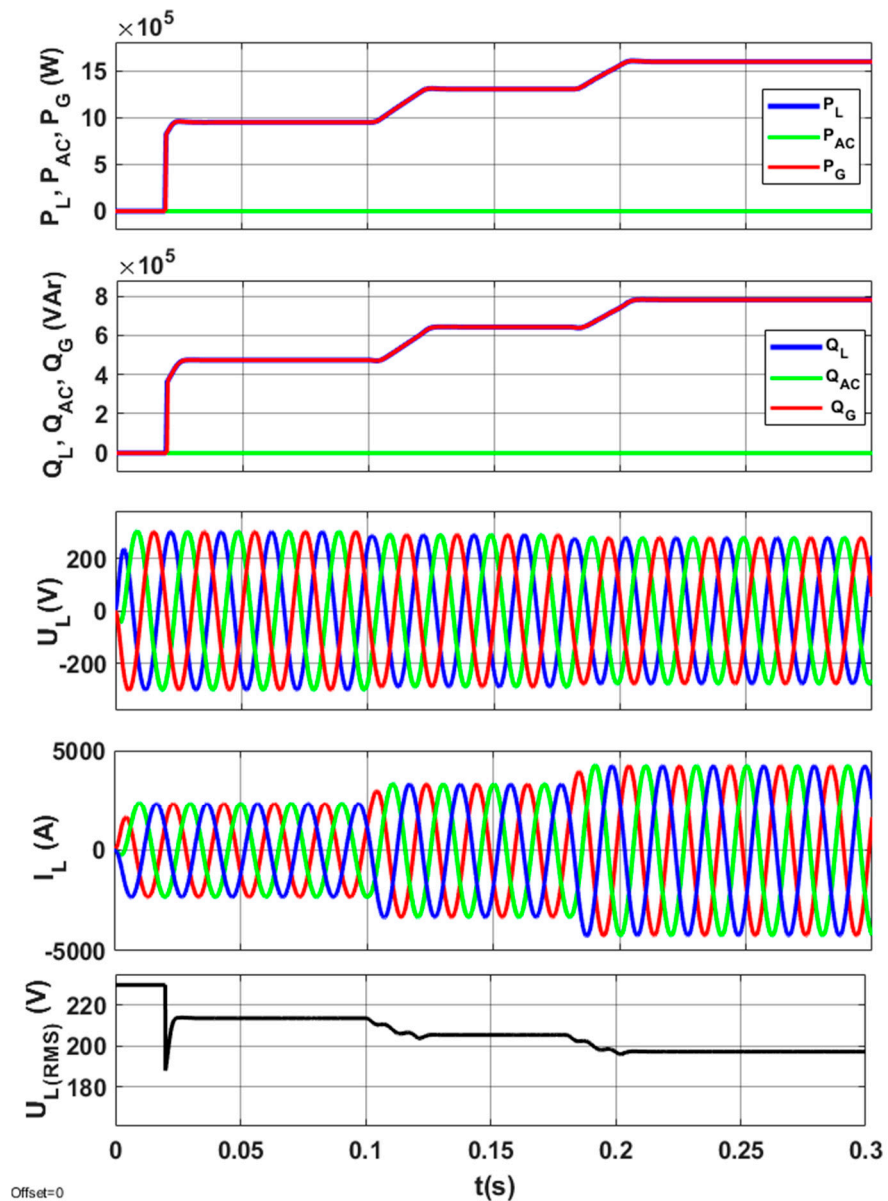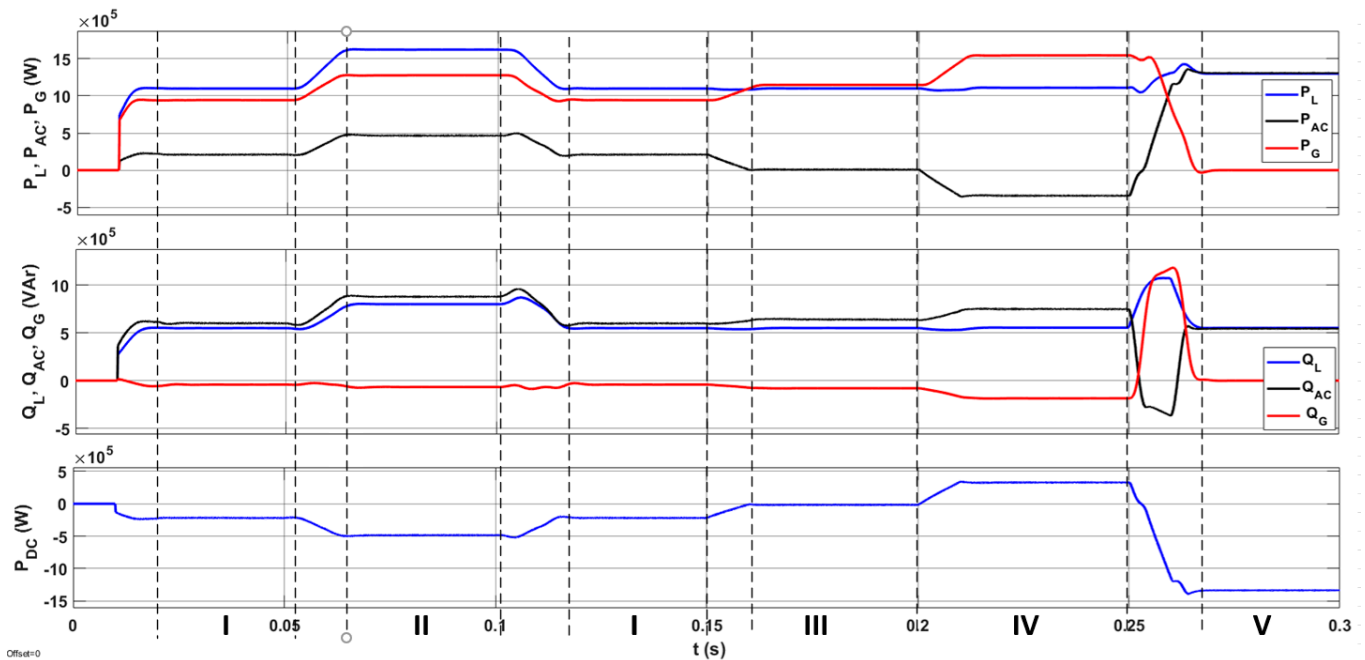

Figure 13. Energy and electromagnetic processes without AC operation: waveforms of active power on the load, generator, and AC (P_L, P_G, P_{AC}); reactive power on the load, generator, and AC (Q_L, Q_G, P_{AC}); and voltage on the load (U_L).

The energy and electromagnetic processes of the D-PMSG set (without AC operation) shown in Figure 13 illustrate the lack of voltage stabilization when increasing the load, which is obvious in the lack of AVR (automatic voltage regulator) in the PMSG. At the same time, the results confirm the validity of the hybrid layout of the ship power plant in parallel topology proposed in the article. At AC failure, the voltage drop at maximum load is about 17% and is within the limit allowed by the regulations of classification societies (20%).

Figures 14 and 15 show energy and electromagnetic processes in a system in which AC control is carried out in accordance with Equations (5), (9) and (10).

Figure 14. Energy processes with AC operation: waveforms of active power on the load, generator, and AC (P_L, P_G, P_{AC}); reactive power on the load, generator, and AC (Q_L, Q_G, P_{AC}), and voltage on the load (U_L).

The hybrid system of the ship's power plant operates in five modes described in the introduction (Figure 14).

I. Ship Maneuvers. The D-PMSG generating set provides active power P_G and additionally, active power P_{AC} is transferred through the electricity storage to the ship network. D-PMSG works at optimal load. The Q_{AC} reactive power is transferred via AC from the electricity storage to the grid and to the PMSG to stabilize the grid's constant voltage U_L ($Q_{AC} = QL + Q_G$).

II. Ship sea voyage—short-term dynamic load increase. The D-PMSG generating set provides active power P_G and additionally increased active power P_{AC} is transferred through the electricity storage to the ship network. The Q_{AC} reactive power is transferred via AC from the electricity storage to the grid and to the PMSG to stabilize the grid's DC voltage U_L ($Q_{AC} = QL + Q_G$).

III. Sea voyage of the ship—stable load of the power plant. The D-PMSG generating set gives P_G active power to the ship's grid ($P_G = P_L$). The energy store is not discharged ($P_{AC} = 0$). The Q_{AC} reactive power is transferred via AC from the electricity storage to the grid and to the PMSG to stabilize the grid's DC voltage U_L ($Q_{AC} = QL + Q_G$).

IV. Ship's sea voyage—stable power plant load and battery charging (if necessary). The D-PMSG generating set gives P_G active power to the grid and to the electricity storage, charging the batteries ($P_G = P_L + P_{AC}$). Reactive power Q_{AC} via AC from

the electricity storage is transferred from the AC to the grid and to the PMSG to stabilize the DC voltage of the grid U_L ($Q_{AC} = QL + Q_G$).

V. Stay in port—D-PMSG power generator is switched off. Active power P_{AC} and reactive power Q_{AC} is transferred via AC from the electricity storage ($P_{AC} = P_L$, $Q_{AC} = Q_L$).
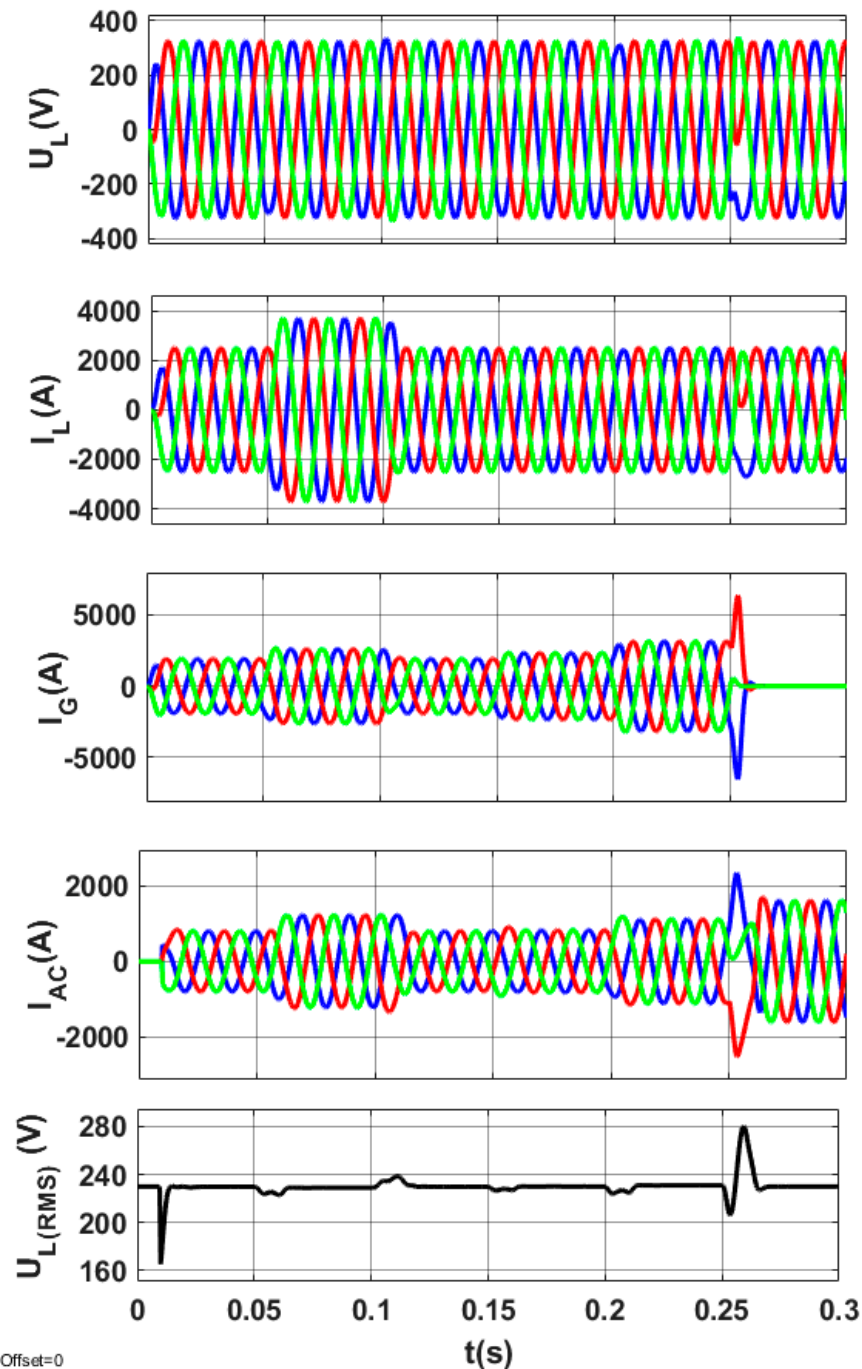
Figure 15. Electromagnetic processes in the system with AC operation.

Figure 14 shows the energy processes in the analyzed hybrid system with decoupled control of the AC power so as to ensure optimal energy management in the ship's grid while stabilizing the grid voltage

In mode I, parallel operation (maneuvering) is required for safety. The active power load of the D-PMSG and battery storage is asymmetric to ensure the smallest SFC for the

internal combustion engine of the PMSG drive [34]. In mode II (ship sea voyage), the active power output of the D-PMSG and energy storage increases when a significant load is switched on briefly. In mode III (ship sea voyage), active power is only given off by the D-PMSG, and the battery storage is not discharged. In mode IV, the active power of the P_{AC} is negative—the storage is charged. In mode V, the D-PMSG is disconnected (port stop) and the active power of P_{AC} and reactive power of Q_{AC} are given back to the grid. AC control in this mode is standard.

In all modes of operation of the system, except in V mode where the reactive power is given by the AC only to the load (D-PMSG unit disconnected), the PMSG is capacitively loaded (negative reactive power Q_G) to stabilize the network voltage.

Based on Figures 13 and 15, it is possible to make a comparison of the electromagnetic characteristics of the system operation during load change without PMSG armature compensation and with armature compensation with the AC. From the comparison of test results, it can be seen that the proposed system achieved effective compensation of the voltage (U_L) drop with the load change.

Figure 15 shows transients between vessel modes, where small overshoots (e.g., $U_{L(RMS)} = f(t)$) are visible. This is due to the fact that the adopted control algorithm is based on static-state analysis.

4. Discussion and Conclusions

Ship systems using battery storage in autonomous or hybrid systems to reduce air pollutant emissions are primarily proposed for the ship's electric drive [41,42]. The main disadvantage of such a solution is that it can be used only for low-power propulsion engines (small ships). The limitations are related to the weight, volume, and cost of the batteries. The autonomous hybrid system for ship power plants proposed in this article allows for the use of this solution on all types of ships (except for large passenger ships, where the power of the power plant may exceed even 10 MW).

The analysis of the feasibility of implementing an autonomous hybrid power plant system consisting of a D-PMSG generating set and a battery energy storage presented in this article was confirmed in model tests.

The contribution of the solution proposed in this paper is, therefore, as follows:

- In the analyzed power plant system, replacing the commonly used EESG generator with the PMSG generator increases the efficiency of the power plant system (especially for small loads), which is a result of the properties of the PMSG. The innovative algorithm of decoupled AC power control enables voltage stabilization in the ship power grid in all power plant operating modes.
- The use of the proposed hybrid ship power plant system in comparison with the classic (serial topology) power plant system with the PMSG increases the reliability of the power plant system. The proposed parallel topology of the hybrid marine power plant system (Figure 2) allows, in the event of a converter failure, operation by the ship's crew by enabling uninterrupted switching to the second generating set, which is impossible in commonly used series systems (Figure 1).
- Decoupled active and reactive power flow control (PAC and QAC) ensures the implementation of the system operating modes presented in the article, improving the energy efficiency of the power plant system:
  - Mode I: in classic solutions, two D-G units work in parallel, symmetrically with a low unit load (high specific fuel consumption coefficient (k_e)) [34]. In the proposed solution, the D-PMSG unit is optimally loaded (k_e is minimal).
  - Mode II: in classic solutions, for the power demand, the second D-G generating set is switched on for parallel operation. In the proposed solution, one D-G unit and an electricity storage facility operate in this mode of operation.
- The proposed hybrid system of the ship's power plant enables switching off the generating sets during a stay in the port and using the electricity storage installed in the system (V mode). It is an alternative system to the universal "Shore To Ship"

system, which is not always available at the port. The proposed system can also be used as a universal "Shore To Ship" system, i.e., connection of shore power supply, regardless of the voltage level and frequency, by connecting the power supply through a matching transformer and an active rectifier to the AC intermediary circuit.

The reduction in specific fuel consumption of the proposed hybrid ship power plant system presented in this article, compared with commonly used solutions, results in economic (lower fuel consumption) and, at the same time, environmental benefits in both sea voyage and ship maneuvering modes.

Most of the used AC control methods based on steady-state analysis are characterized by a complicated control algorithm. In the AC control based on steady-state analysis proposed in this article, the load on the processor (computing) unit is low.

The disadvantage of methods based on steady-state analysis is the lack of transient control. The authors are currently working on a new AC control algorithm based on the PMSG I/O linearization technique [43] to enable control of the system operation during transients, which will be presented in the next article.

Currently, the authors are in the process of building a laboratory stand from a hybrid power plant with the PMSG based on a new technology, i.e., the Speedgoat module [44]. It should be noted here that the simulation models used in the article and developed in Matlab-Simulink can be easily used during laboratory experiments because the Speedgoat module is 100% compatible with Matlab-Simulink. In the next article, the authors will present the experimental results.

5. Patents

German-Galkin, S.; Tarnapowicz, D. Method and system of stabilizing the frequency and voltage of autonomous power generating units. Patent Office of the Republic of Poland, Patent PL241441, al. Niepodległości 188/192, 00-950 Warszawa, 2020.

Author Contributions: Conceptualization, A.N., D.T., S.G.-G. and M.J.; methodology, A.N., D.T. and S.G.-G.; validation, D.T. and S.G.-G.; formal analysis, A.N., D.T. and S.G.-G.; investigation, A.N., D.T. and S.G.-G.; writing—original draft preparation, A.N., D.T. and S.G.-G.; writing—review and editing, D.T. and S.G.-G. All authors have read and agreed to the published version of the manuscript.

Data Availability Statement: Not applicable.

References

1. Nicewicz, G.; Sosinski, M.; Tarnapowicz, D. Identification of Power Factor in Marine Electrical Grid. In Proceedings of the 14th International Multidisciplinary Scientific Geoconference (SGEM), Albena, Bulgaria, 17–26 June 2014; pp. 391–398, ISBN 978-619-7105-16-2.
2. Polakis, M.; Zachariadis, P.; Kat, J.O. The Energy Efficiency Design Index (EEDI). In *Sustainable Shipping*; Springer: New York, NY, USA, 2019; pp. 93–135. [CrossRef]
3. International Maritime Organization. *IMO Train the Trainer (TTT) Course on Energy Efficiency Ship Operation. Module 2—Ship Energy Efficiency Regulations and Related Guidelines*; International Maritime Organization: London, UK, 2016; Available online: https://www.cdn.imo.org/localresources/en/OurWork/Environment/Documents/Air%20polltion/TTT%20trainers%20manual%20final2.pdf (accessed on 5 May 2022).
4. The Switch. Yaskawa Company. Available online: https://theswitch.com/marine/ (accessed on 1 October 2022).
5. ABB. Permanent Magnet Shaft Generators Improve Vessel Energy Efficiency. Available online: https://new.abb.com/news/detail/96712/permanent-magnet-shaft-generators-improve-vessel-energy-efficiency-inside-marine-article (accessed on 1 October 2022).
6. Cheng, H.; Chen, H.; Wang, Q. An Integrated Drive Power Converter Topology for Plug-in Hybrid Electric Vehicle with G2V, V2G and V2H Functions. In Proceedings of the 2019 22nd International Conference on Electrical Machines and Systems (ICEMS), Harbin, China, 11–14 August 2019; pp. 1–6. [CrossRef]
7. Jindo, S.; Kondo, K.; Kondo, M.; Yokouchi, T. Power Generation Control Method of Parallel Resonant PMSG System for Series Hybrid Vehicle. In Proceedings of the 2022 International Power Electronics Conference (IPEC-Himeji 2022-ECCE Asia), Himeji, Japan, 15–19 May 2022; pp. 1878–1884. [CrossRef]

8. Chauhan, A.K.; Vakacharla, V.R.; Verma, A.K.; Singh, S.K. Multiple PMSG fed Non-Inverting Buck-Boost Converter for HEVs. In Proceedings of the 2016 IEEE 6th International Conference on Power Systems (ICPS), New Delhi, India, 4–6 March 2016; pp. 1–6. [CrossRef]

9. Hassan, S.Z.; Li, H.; Kamal, T.; Awais, M. Stand-Alone/Grid-Tied Wind Power System with Battery/Supercapacitor Hybrid Energy Storage. In Proceedings of the 2015 International Conference on Emerging Technologies (ICET), Peshawar, Pakistan, 19–20 December 2015; pp. 1–6. [CrossRef]

10. Wei, J.; Wang, Y.; Wen, X.; Li, H.; Zhang, Y.; Li, K. A New Control Method for Microturbine-generation based Series Hybrid Power System. In Proceedings of the 2019 22nd International Conference on Electrical Machines and Systems (ICEMS), Harbin, China, 11–14 August 2019; pp. 1–5. [CrossRef]

11. Nayak, S.K.; Vinod, H. Performance Study of Common DC Link Connected Wind and PV Hybrid System. In Proceedings of the 2016 IEEE 7th Power India International Conference (PIICON), Bikaner, India, 25–27 November 2016; pp. 1–5. [CrossRef]

12. Giangrande, P.; Madonna, V.; Sala, G.; Kladas, A.; Gerada, C.; Galea, M. Design and Testing of PMSM for Aerospace EMA Applications. In Proceedings of the IECON 2018—44th Annual Conference of the IEEE Industrial Electronics Society, Washington, DC, USA, 20–23 October 2018; pp. 2038–2043. [CrossRef]

13. Wang, C.; Yang, T.; Hussaini, H.; Huang, Z.; Bozhko, S. Power Quality Improvement Using an Active Power Sharing Scheme in More Electric Aircraft. *IEEE Trans. Ind. Electron.* **2022**, *69*, 3588–3598. [CrossRef]

14. Lucjan, S.; Rafał, K. The Study of Permanent Magnets Synchronous Machine (PMSM) of the Autonomous Electric Power Supply System (ASE), Compatible with the Concept of a More Electric Aircraft (MEA). In Proceedings of the International Conference on Applied Mathematics, Computational Science and Systems Engineering, TM Web of Conferences, Athens, Greece, 6–8 October 2017; Volume 16.

15. Sarigiannidis, A.G.; Chatzinikolaou, E.; Patsios, C.; Kladas, A.G. Shaft Generator System Design and Ship Operation Improvement Involving SFOC Minimization, Electric Grid Conditioning, and Auxiliary Propulsion. *IEEE Trans. Transp. Electrif.* **2016**, *2*, 558–569. [CrossRef]

16. Accetta, A.; Pucci, M. Energy Management System in DC Micro-Grids of Smart Ships: Main Gen-Set Fuel Consumption Minimization and Fault Compensation. *IEEE Trans. Ind. Appl.* **2019**, *55*, 3097–3113. [CrossRef]

17. German-Galkin, S.; Tarnapowicz, D.; Matuszak, Z.; Jaskiewicz, M. Optimization to Limit the Effects of Underloaded Generator Sets in Stand-Alone Hybrid Ship Grids. *Energies* **2020**, *13*, 708. [CrossRef]

18. German-Galkin, S.; Tarnapowicz, D. Energy Optimization of the 'Shore to Ship' System-A Universal Power System for Ships at Berth in a Port. *Sensors* **2020**, *20*, 3815. [CrossRef] [PubMed]

19. Singaravel, M.M.R.; Daniel, S.A. MPPT With Single DC–DC Converter and Inverter for Grid-Connected Hybrid Wind-Driven PMSG–PV System. *IEEE Trans. Ind. Electron.* **2015**, *62*, 4849–4857. [CrossRef]

20. Singh, B.; Niwas, R.; Dube, S.K. Load Leveling and Voltage Control of Permanent Magnet Synchronous Generator-Based DG Set for Standalone Supply System. *IEEE Trans. Ind. Inform.* **2014**, *10*, 2034–2043. [CrossRef]

21. Jain, A.; Saravanakumar, R. Comparative Analysis of DSOGI-PLL& Adaptive Frequency Loop-PLL for Voltage and Frequency Control of PMSG-BESS based Hybrid Standalone WECS. In Proceedings of the 2018 8th International Conference on Power and Energy Systems (ICPES), Colombo, Sri Lanka, 21–22 December 2018; pp. 234–239. [CrossRef]

22. Sharma, P.; Sharma, C. Automatic Reactive Power Compensation of an Isolated Wind-Diesel Hybrid Grid. In Proceedings of the 2018 IEEE International Conference on Industrial Technology (ICIT), Lyon, France, 19–22 February 2018; pp. 1171–1176. [CrossRef]

23. Singh, B.; Niwas, K. Power Quality Improvement of PMSG based DG Set Feeding 3-Phase 3-Wire Load. In Proceedings of the 2014 IEEE International Conference on Power Electronics, Drives and Energy Systems (PEDES), Mumbai, India, 16–19 December 2014; pp. 1–6. [CrossRef]

24. German-Galkin, S.; Tarnapowicz, D. Method and System of Stabilizing the Frequency and Voltage of Autonomous Power Generating. Units. Patent PL241441, 10 March 2020.

25. Yang, X.; Bai, G.; Schmidhalter, R. Shore to Ship Converter System for Energy Saving and Emission Reduction. In Proceedings of the8th International Conference on Power Electronics—ECCE Asia, Jeju, Republic of Korea, 30 May–3 June 2011; pp. 2081–2086. [CrossRef]

26. Tarnapowicz, D. Load Analysis of Ship Generating Sets During the Maneuvers of the Vessel. In *Current Methods of Construction Design, Proceedings of the 59th International Conference of Machine Design Departments (ICMD), Demanovska Dolina, Slovakia, 11–14 September 2018*; Springer: Cham, Switzerland, 2018; pp. 399–407. [CrossRef]

27. Patel, D.K.; Singh, D.; Singh, B. Impact assessment of distributed generations with electric vehicles planning: A review. *J. Energy Storage* **2021**, *43*, 103092. [CrossRef]

28. Patel, D.K.; Singh, D.; Singh, B. Genetic algorithm-based multi-objective optimization for distributed generations planning in distribution systems with constant impedance, constant current, constant power load models. *Int. Trans. Electr. Energy Syst.* **2020**, *30*, e12576. [CrossRef]

29. Singh, B.; Sharma, J. A review on distributed generation planning. *Renew. Sustain. Energy Rev.* **2017**, *76*, 529–544. [CrossRef]

30. Singh, B.; Pal, C.; Mukherjee, V.; Tiwari, P.; Yadav, M.K. Distributed generation planning from power system performances viewpoints: A taxonomical survey. *Renew. Sustain. Energy Rev.* **2017**, *75*, 1472–1492. [CrossRef]

31. Borkar, P.; Kumar, N.; Choudhary, D. Active Power Rescheduling of Generator for Congestion Management using Whale Optimization Technique. In Proceedings of the 2018 International Conference on Smart Electric Drives and Power System (ICSEDPS), Nagpur, India, 12–13 June 2018; pp. 142–146. [CrossRef]

32. Gad, Y.; Diab, H.; Abdelsalam, M.; Galal, Y. Smart Energy Management System of Environmentally Friendly Microgrid Based on Grasshopper Optimization Technique. *Energies* **2020**, *13*, 5000. [CrossRef]

33. Shahzad, M.; Akram, W.; Arif, M.; Khan, U.; Ullah, B. Optimal Siting and Sizing of Distributed Generators by Strawberry Plant Propagation Algorithm. *Energies* **2021**, *14*, 1744. [CrossRef]

34. Cuculic, A.; Vucetic, D.; Prenc, R.; Celic, J. Analysis of Energy Storage Implementation on Dynamically Positioned Vessels. *Energies* **2019**, *12*, 444. [CrossRef]

35. MAN. Batteries on Board Ocean-Going Vessels. Available online: https://www.man-es.com/docs/default-source/marine/tools/batteries-on-board-ocean-going-vessels.pdf?sfvrsn=deaa76b8_14 (accessed on 1 October 2022).

36. German-Galkin, S. MATLAB School: Lesson 24. In *Mechatronic System with Magnetoelectric Generator and Active Semiconductor Rectifier*; Magazine "Power Electronics" No.1(70); Power-e: St-Petersburg, Russia, 2018; pp. 6–13.

37. Brodsky, V.N.; Ivanov, E.S. *Frequency-Controlled Drives*; Energy: Moscow, Russia, 1974; p. 168.

38. Rozanov, Y.K.; Ryabchiiskii, M.V.; Kvasyuk, A.A. *Power Electronics*; MPEI Publishing House: Moscow, Russia, 2007; p. 632.

39. Gorev, A. *Transient Processes of Synchronous Machine*; State Energy Publishing House (Gosenergoizdat): Leningrad, Russia, 1950.

40. Park, R.H. Two-reaction theory of synchronous machines-II. *Trans. Am. Inst. Electr. Eng.* **1933**, *52*, 352–354. [CrossRef]

41. Jayasinghe, S.G.; Suryawanshi, U.; Sheikh, A.; Alahakoon, S. Fuel Saving with a Hybrid Power System for an Electric Ferry. In Proceedings of the 2019 14th Conference on Industrial and Information Systems (ICIIS), Kandy, Sri Lanka, 18–20 December 2019; pp. 255–259. [CrossRef]

42. Yang, R.; Jiang, L.; Du, K.; Zhang, Y.; Wang, L.; Li, K. Research and Experimentation on Energy Management System for Inland Diesel-Electric Hybrid Power Ships. In Proceedings of the 2020 IEEE 8th International Conference on Computer Science and Network Technology (ICCSNT), Dalian, China, 20–22 November 2020; pp. 102–106. [CrossRef]

43. Zwierzewicz, Z.; Tarnapowicz, D.; German-Galkin, S.; Jaskiewicz, M. Optimal Control of the Diesel–Electric Propulsion in a Ship with PMSM. *Energies* **2022**, *15*, 9390. [CrossRef]

44. Speedgoat. Rapid Control Prototyping. Available online: https://www.speedgoat.com/solutions/testing-workflows/rapid-control-prototyping (accessed on 12 December 2022).